Bulletin of the Geological Survey of Japan, vol. 31(7), p. 321–332, 1980 551.2: 550.36: 681.3

Numerical Model Experiment of Hydrothermal System —Topographic Effects—

Naoyuki HANAOKA*

HANAOKA, N. (1980) Numerical model experiment of hydrothermal system—Topographic effects—. *Bull. Geol. Surv. Japan*, vol. 31(7), p. 321–332.

Abstract: Numerical models are developed to analyse topographic effects on hydrothermal system in homogeneous medium. Water table is assumed to coincide with ground surface.

A moderate mountain above heat source acts as a cap for geothermal system which stores large amount of heat. The convection pattern of thermal fluid at depth may change completely, when the height of the mountain exceeds a certain critical level.

Vertical temperature profiles obtained from the numerical models show many features we encounter in field data such as a steep thermal gradient at intermediate level and a temperature reverse, and make it possible to interprete field temperature logs in terms of a supposed geothermal system.

Introduction

With increasing interest in geothermal energy, exploration activities sponsored by central government and private undertakings have become high. In these works, many varied exploration techniques are applied including those which have developed in other exploration fields such as a mining and oil industries. So, it is not rare to find many kinds of exploration and research data for a promising field. For more accurate assessment of geothermal resource, it is indispensable to integrate all these data into one model which can explain the characteristics in the data reasonably. This study is a part of efforts for making up physical images of geothermal reservoir under regional perspective.

It has been noticed that shallow heat hole measurements are strongly perturbed by ground water movement. As to the relation between geothermal system and regional ground water flow, HEALY (1975) noticed that most large hot water systems are located in discharge areas in basins or valleys, and proposed the diagrams illustrating concentration of heat by ground water of which no convection was taken into account.

Recently well developed numerical modeling technique is applied in this study to analyse the interaction between hydrological fluid flow and convection flow. As preliminary study, no real field data are simulated. Models are rather simple and idealistic, but enough to demonstrate the general pattern of hot and cold fluid flows under the effects of heat and fluid potential.

It is reported that the level of ground water follows the ground surface very well (GUSTAFSSON, 1968) in a plain. But little is known about the surface of ground water in mountaineous volcanic area. It seems not unrealistic to assume that the surface of ground water may be some how estimated from the ground surface when precipitation can be expected throughout the year.

Numerical Models

The governing equations of single phase steady state hydrothermal system have been given by many authors (e.g. DONALDSON, 1962). Here, we use the simplified equations of those given by FAUST and MERCER (1979), i. e.,

*Geothermal Research Department

for mass balance,

$$\nabla\cdot\left[\frac{\mathbb{K}\rho}{\mu}\cdot(\nabla p-\rho g\nabla D)\right]+q_m=0 \qquad (1)$$

and for energy balance,

$$\nabla\cdot\left[\frac{\mathbb{K}\rho h}{\mu}\cdot(\nabla p-\rho g\nabla D)\right] +\nabla\cdot\left[K_m\left(\frac{\partial T}{\partial h}\right)_p\nabla h\right]+q_h=0 \qquad (2)$$

where $\mathbb{K}$ is the intrinsic permeability tensor of the porous medium, ρ and μ are the density and dynamic viscosity of water respectively, p is the pressure of fluid, g is the gravitational constant, D is the depth, h is the fluid enthalpy, K_m is the thermal conduction-dispersion coefficient, and q_m and q_h are source terms for mass and energy.

These differential equations are transformed to simultaneous linear equations by employing the Galerkin finite element method (ZIENKIEWICZ, 1971), and solved for pressure and enthalpy or temperature.

The density of fluid is assumed to depend only on temperature by the following equation (MERCER *et al.*, 1975),

$$\rho = \rho_0 - aT - bT^2$$
$$\rho_0 = 1006.06$$
$$a = 0.24602$$
$$b = 0.00231633$$

where T is in degree Celsius and ρ in kg/m^3. Although this equation is valid for the liquid saturation temperatures between 100° and 280°C, it is used in this study for temperature range from 0° to 300°C. The discrepancy of this empirical formula from the values from the steam table (JSME, 1968) is given in Figure 1.

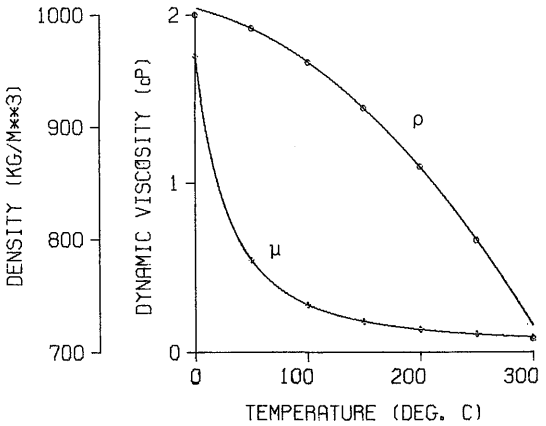

Fig. 1 Empirical curves used in this study and values from the steam table (JSME, 1968) for density ρ (upper line) and dynamic viscosity μ (lower line).

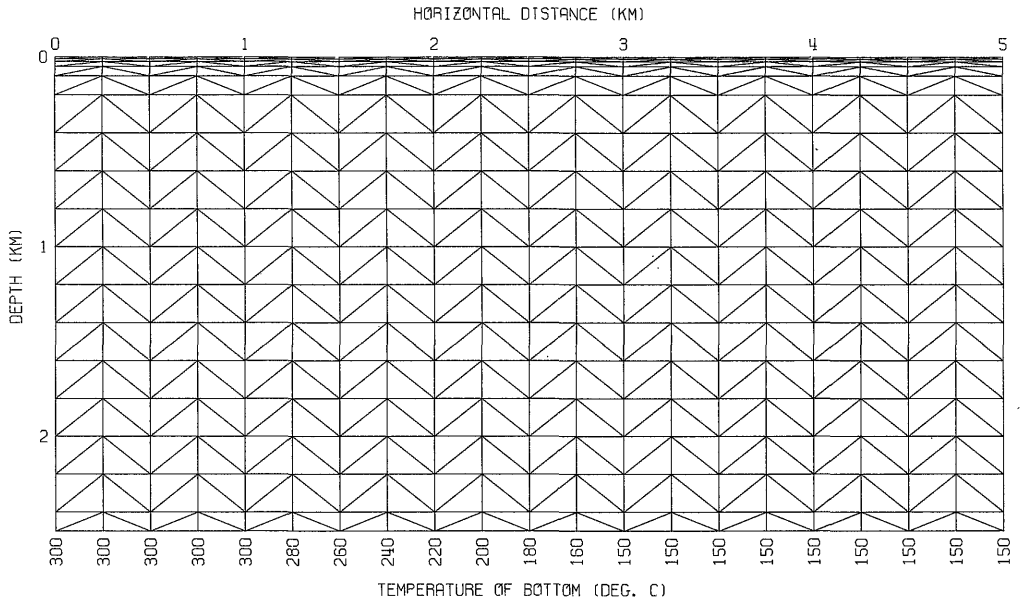

Fig. 2 Finite element net with its supposed size and the fixed values of temperature on the bottom.

The dynamic viscosity μ is a function of temperature and pressure. But for simplicity, we obtain the following formula by neglecting the pressure term of empirical equation (JSME, 1968),

$$\mu = a \times 10^b$$
$$a = 241.4$$
$$b = 247.8/(T + 133.15) - 7.$$

where μ is in kg/(m· s) or 10^3 cP and T in degree Celsius. This expression is correct on the saturation line.

Fluid enthalpy h is a function of temperature given by

$$h = cT$$

where c is the specific heat of water, and treated as a constant value of 4.18605×10^3 J/(kg· °C) for all temperature range.

Two dimensional structures are studied assuming physical characteristics are uniform along the horizontal direction denoted by y-axis. The computation space of homogeneous isotropic medium is divided into meshes. Each quadrangle is further subdivided into two triangular elements. The basic computation space is shown in Figure 2. The size of the space is supposed to be 5 km in horizontal x direction and 2.5 km in vertical direction z. The nodal points along the horizontal x-axis are equally spaced with the interval of 250 m. Whereas, along the vertical axis, the depth of nodal points are as follows, 0, 10, 25, 50, 100, 200, 400, 600, 800, 1000, 1200, 1400, 1600, 1800, 2000, 2200, 2400, and 2500 m. The number of nodal points are 21 in horizontal direction and 18 in vertical direction. Its total is 378. The topography is given on top of the upper boundary, and the nodal points along vertical line are redistributed proportionally to the values mentioned above.

The temperatures of the upper and lower boundaries are fixed. The surface temperature is uniformly fixed for zero degree Celsius, and the bottom temperature is given in Figure 2, ranging from 300°C on the left to 150°C on the right. The temperature 150°C on the bottom corresponds to the vertical temperature gradient of 0.06°C/m (150°C/2500 m) as the average value.

As the boundary condition for pressure, the constant value of zero Pascal is fixed on the ground surface except one model where fluid pressure at the bottom of a lake is given instead.

The boundaries of both sides are insulating and impermeable to heat and mass respectively. It is equivalent to assume that physical condition is symmetrical with respect to the each boundary. Or, in another word, the computation space corresponds to a half cycle of periodic structure and the left boundary is at the center of heat source.

The porous medium is assumed to be isotropic, and the permeability is treated as a scalar quantity. The values of the permeability and thermal conduction-dispersion coefficient of rock-water mixture is rather arbitrary fixed at 0.3×10^{-14} m² and 3.2 W(m·°C) respectively. These two coefficients governs the relative importance of the first and the second terms

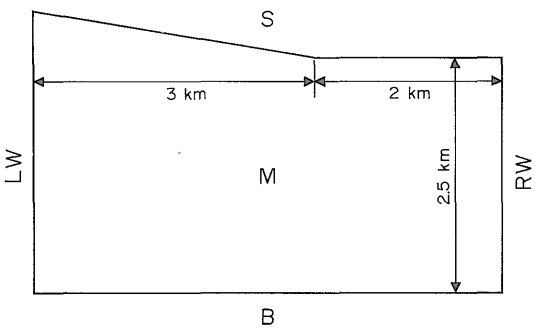

Fig. 3 Boundary conditions and other ones for numerical models.
M; The medium is homogeneous and isotropic. The permeability and thermal conduction-dispersion coefficient are 0.3×10^{-14} m² and 3.2 W/(m·°C) respectively.
S; Topography is given on the surface. Temperature is fixed for 0°C. Pressure is zero Pascal except one model.
B; The temperature on the bottom is fixed as shown in Figure 2. The bottom is impermeable for fluid.
LW, RW; Both side walls are insulating and impermeable for heat and fluid respectively.

of equation (2), i.e. convection and conduction respectively for heat transport. This trade-off relation is yet to be scrutinized incorporating the influence of fluid potential.

The boundary conditions and other ones are summarized in Figure 3.

Results

The topographic effects on hydrothermal system are demonstrated by a series of models in Figure 4. A mountain is placed in the 3 km range on the left just above heat source, and the other part of 2 km on the right remains flat. The slopes of mountains are increased to show the progressively larger effects of fluid potential. The size of flow vector is normalized by the largest vector of each model, and its square root is used for expression without any physical meaning to show the flows in the whole space with reasonably scaled arrows. The isotherms are drawn for 10°C, 100°C, and 200°C.

The model (1) is the basic state with flat ground surface. There is no effect of fluid potential. The vast recharge area and the small discharge area with large mass flux are the results of a convection system.

The moderate slope of gradient 4/100 of model (2) gives the equilibrium condition around the top of the mountain, where flow vectors are very small. The upward force of buoyancy and the downward force due to fluid potential have roughly equal strength at this part. The extended high temperature regime of more than 200°C is apparent as compared to the basic state.

When the gradient of slope is increased, there appear two regimes, cold and hot, in the model (3), of which the gradient of slope is 10/100. There is a parallel flow along the boundary of the two regime. The vertical temperature gradients along this border are large. The maximum gradient of 0.35–0.36°C/m is observed. Heat is transported from the hot regime to the cold regime by conduction-dispersion across this flow. The hot regime of more than 200°C has comparable size as in the model (2). The area of intermediate temperature range between 100°C and 200°C is much extended. These features clearly show that a mountain of appropriate slope above heat source can act as a cap on geothermal convection system.

A further increase of gradient makes little change of the flow system as seen in the model (4). Some of slight changes are as follows. The high temperature zone is reduced due to the expansion of cold regime. The recharge area on the right hand has disappeared. The convection of the models (3) and (4) will be called as a mushroom type after the shape of isotherm hereafter.

A drastic change of flow system is caused by the slight increase of gradient from 17/100 of the model (4) to 18/100 of the model (5). There is a certain critical level of fluid potential where the mushroom type convention system is destroyed and another steady state is produced. The flow pattern of the model (5) is dispersive, and the hot area of more than 200°C is greatly reduced. The low temperature area beneath the mountain is very extensive. The cold water from the high mountain goes down to the bottom of hot plate to be heated.

The effect of the further increase in gradient of slope is the further narrowing of hot zone and the expansion of cold zone of the model (6). The swelling of 100°C isotherm on the right hand seems to be due to the side effect of impermeable boundary.

The vertical temperature profiles of selected columns are shown in Figure 5. Each figure consists of temperature logs from corresponding column of each model described above. The attached numbers correspond to those of the models. For the location of logs, Figure 4 is referenced.

The vertical temperature profiles in Figure 5 (a) are those along side boundary on the left marked as 'a'. As no lateral flow is allowed, the profiles reflect only vertical flow. The profiles 1 and 2 from Figure 4 model (1) and (2) respectively are the temperature in the

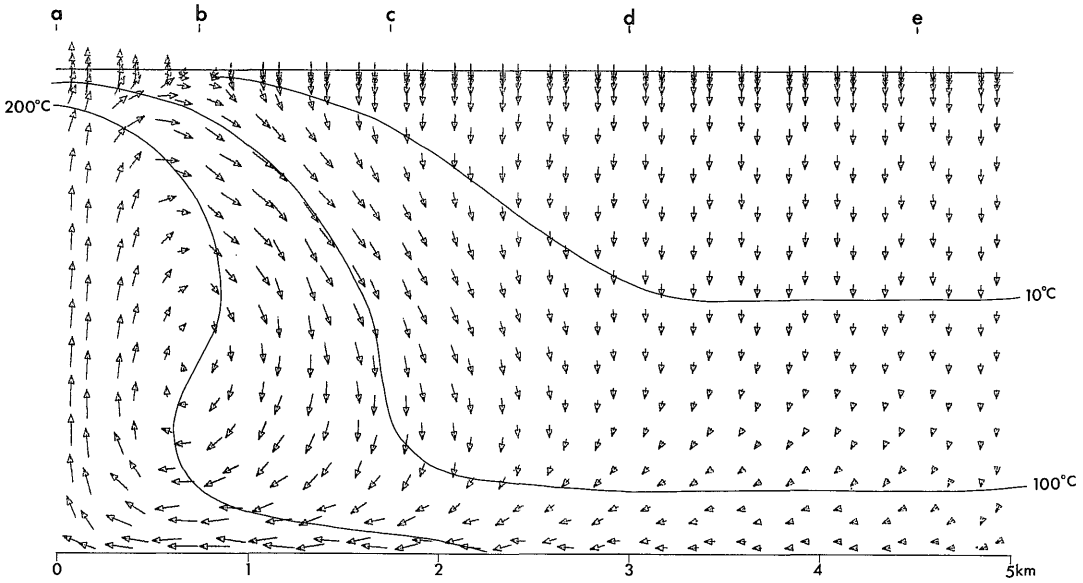

Fig. 4(1)

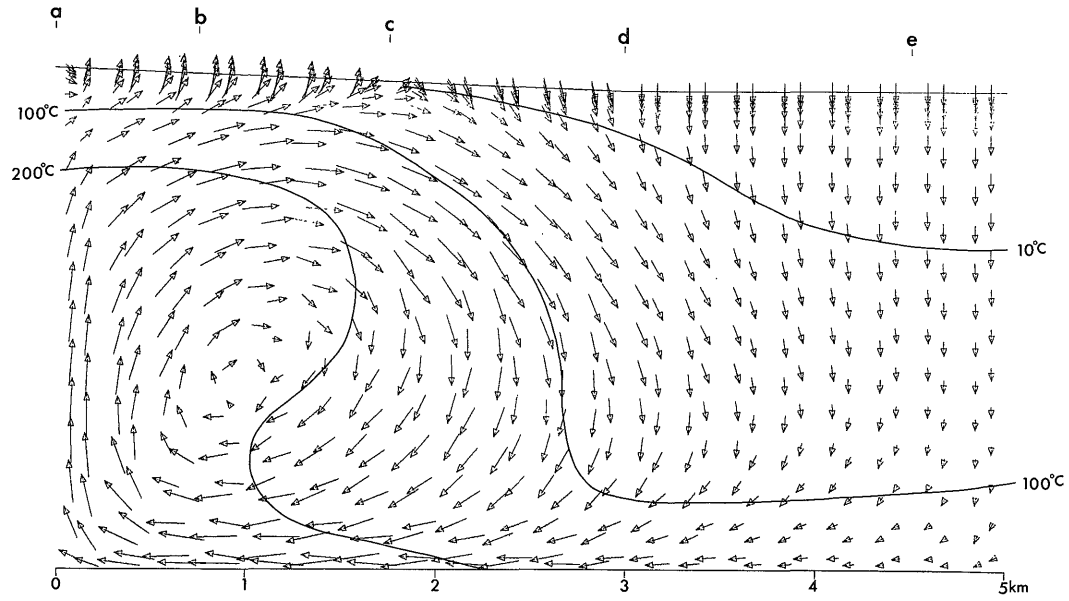

Fig. 4(2)

Fig. 4 Fluid flow vectors normalized by the largest one of each model and presented by its square root. The isotherms are drawn at 10°C, 100°C, and 200°C. The gradients of topographic slopes are as follows, (1) flat (basic state), (2) 4/100 (angle 2.3°), (3) 10/100 (angle 5.7°), (4) 17/100 (angle 9.6°), (5) 18/100 (angle 10.2°), and (6) 30/100 (angle 16.7°).

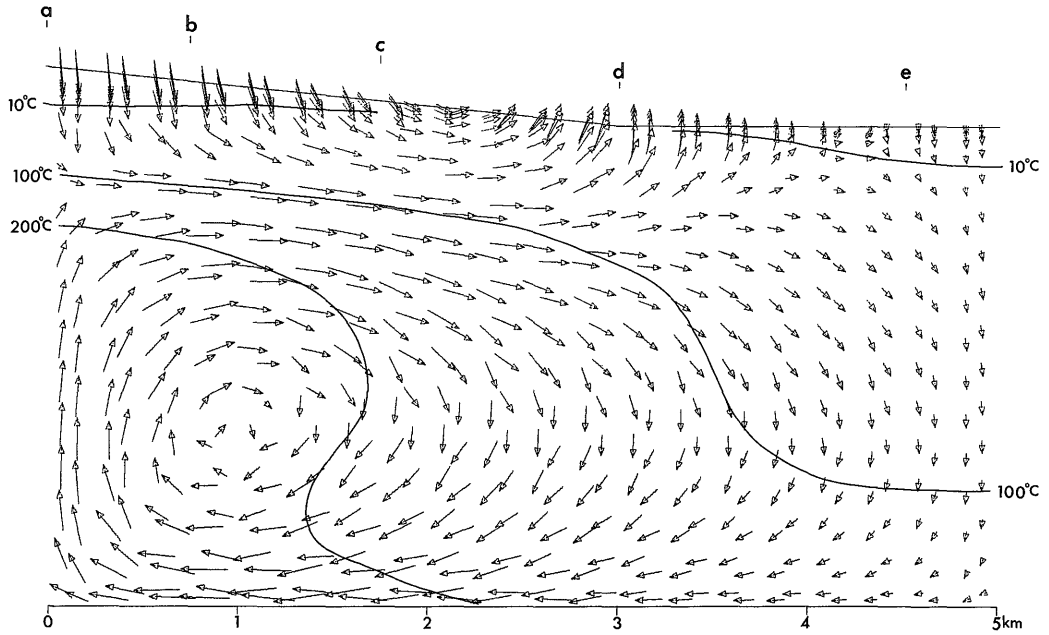
a
b
c
d
e
10°C
100°C
200°C
10°C
100°C
0
1
2
3
4
5km

Fig. 4 (3)

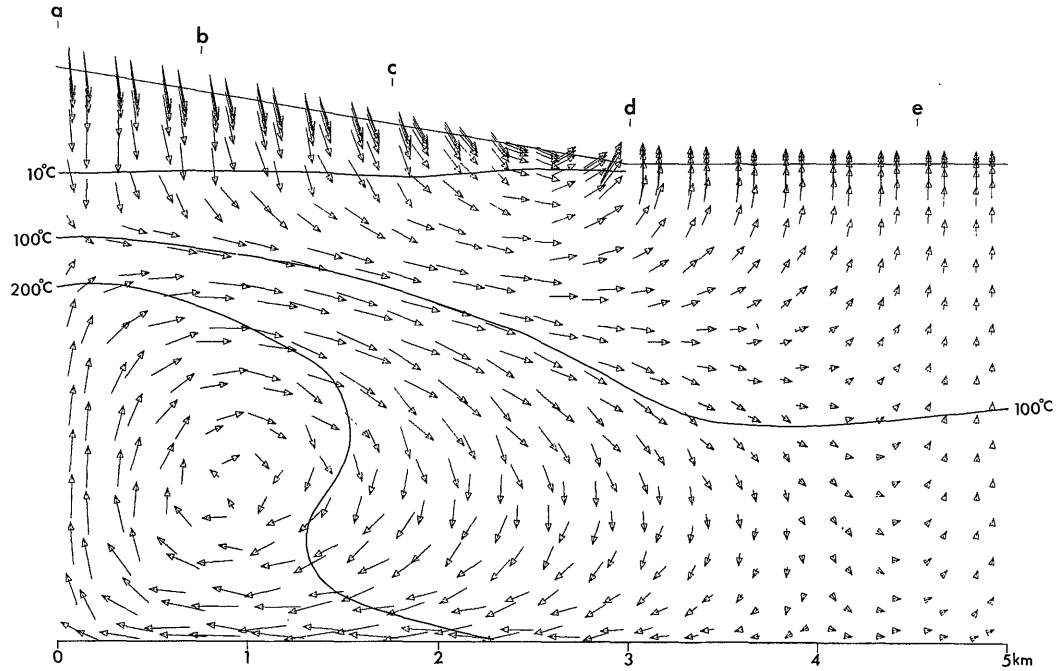
a
b
c
d
e
10°C
100°C
200°C
100°C
0
1
2
3
4
5km

Fig. 4 (4)

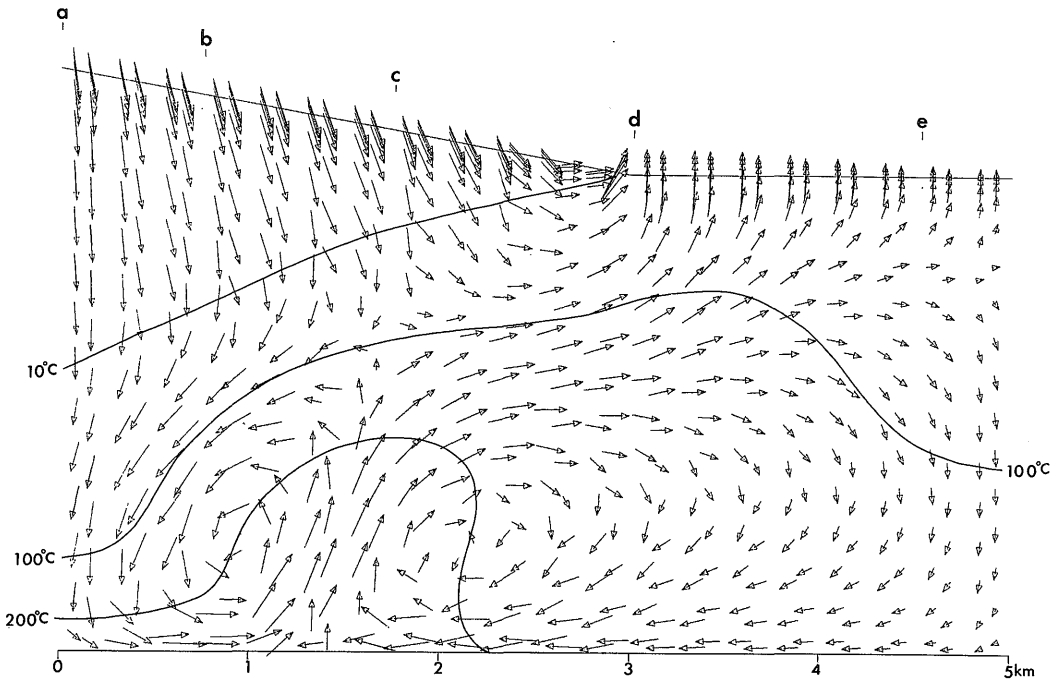
a
b
c
d
e
10°C
100°C
200°C
100°C
0
1
2
3
4
5km

Fig. 4 (5)

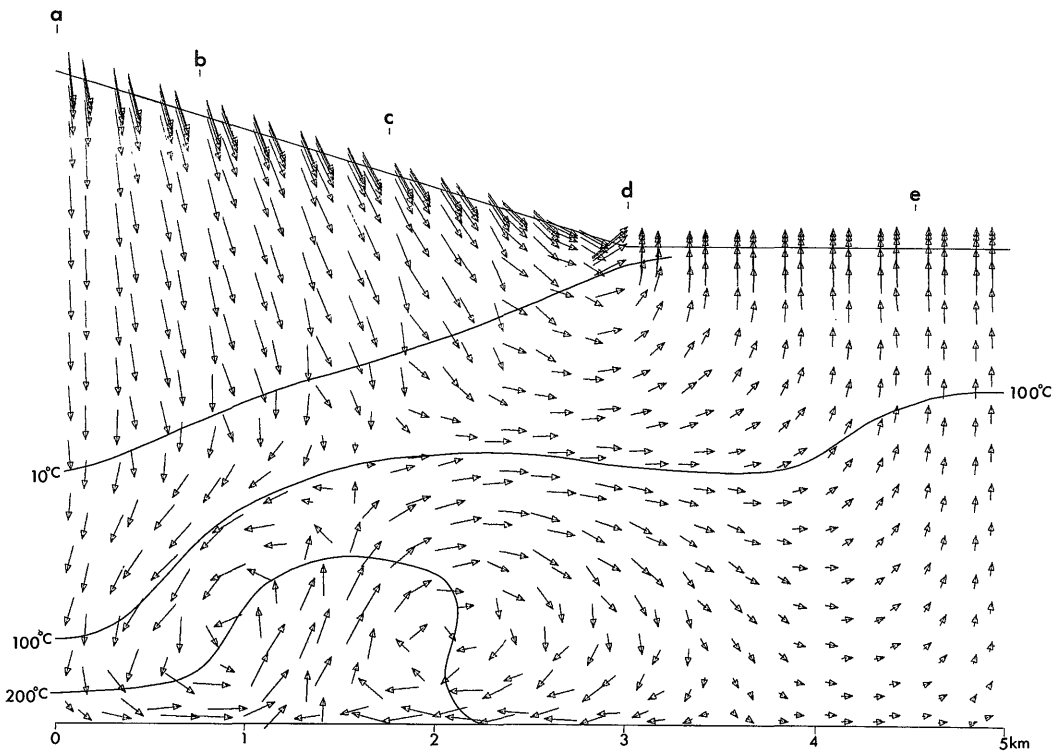
a
b
c
d
e
100°C
10°C
100°C
200°C
0
1
2
3
4
5km

Fig. 4 (6)

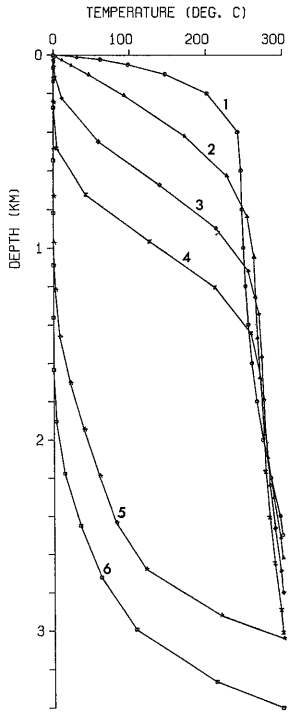

Fig. 5 (a)

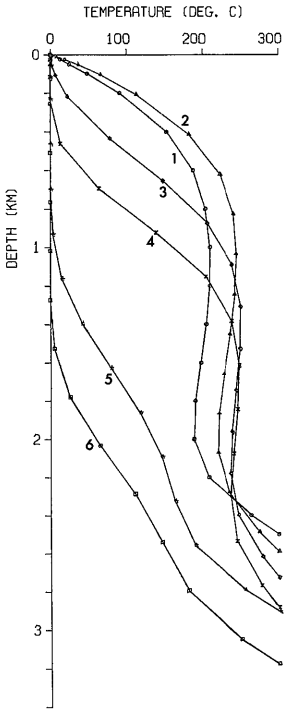

Fig. 5 (b)

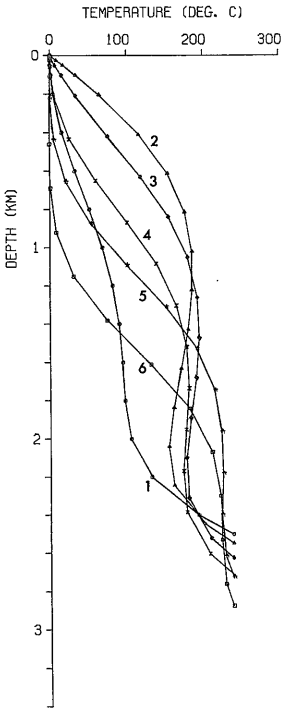

Fig. 5 (c)

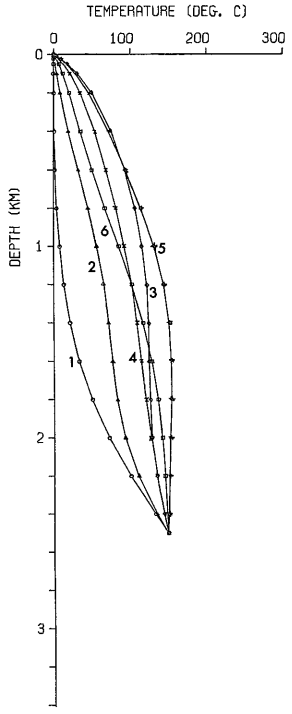

Fig. 5 (d)

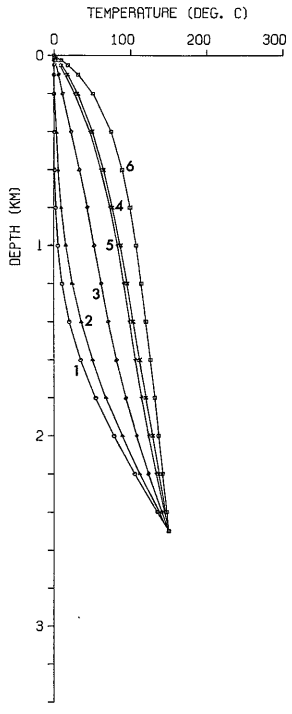

Fig. 5 (e)

Fig. 5 Vertical temperature profiles from models of Figure 4. The locations of temperature log is shown at the models of Figure 4 by symbols a through e.

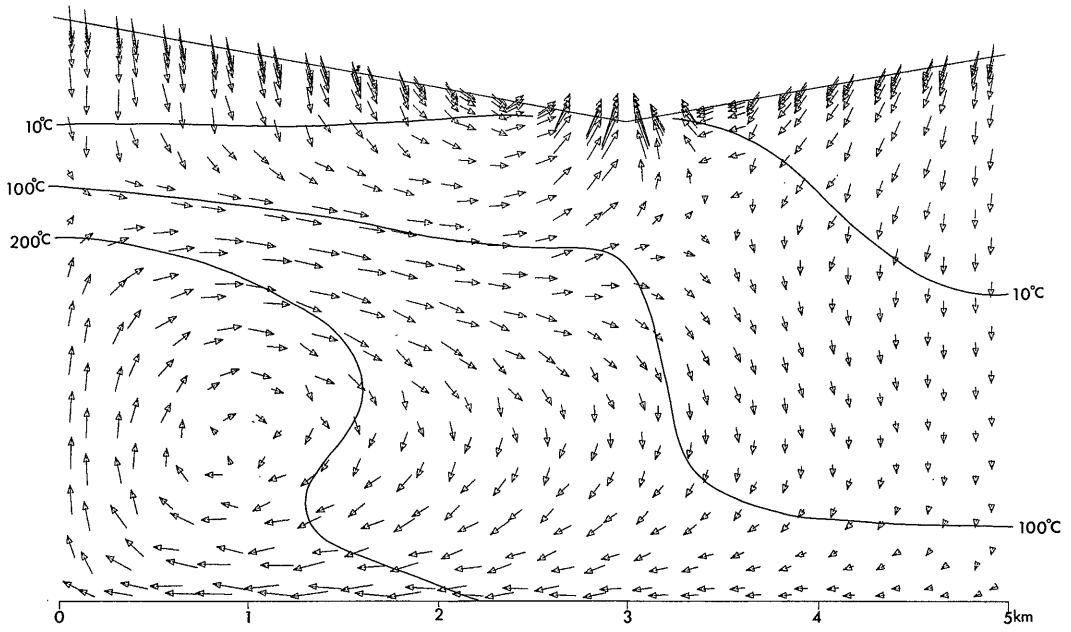

Fig. 6(1)

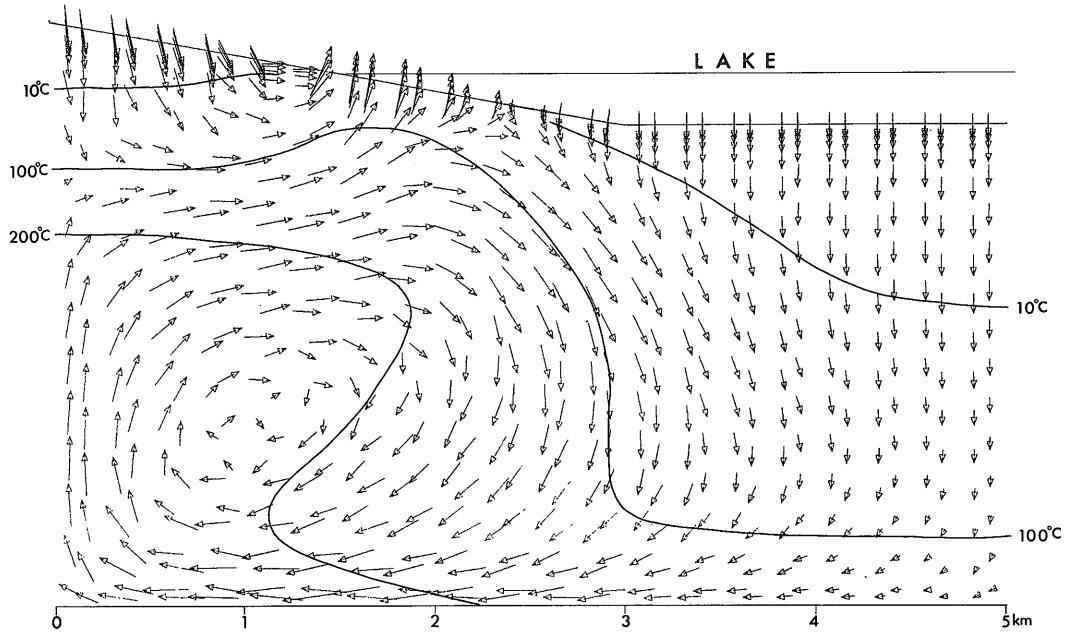

Fig. 6(2)

Fig. 6 Effects of reduced gradient of fluid potential for comparison with the model (5) in Figure 4. (1) A mountain of the same slope is put on the opposite side. (2) A lake is introduced to the middle level of the mountain.

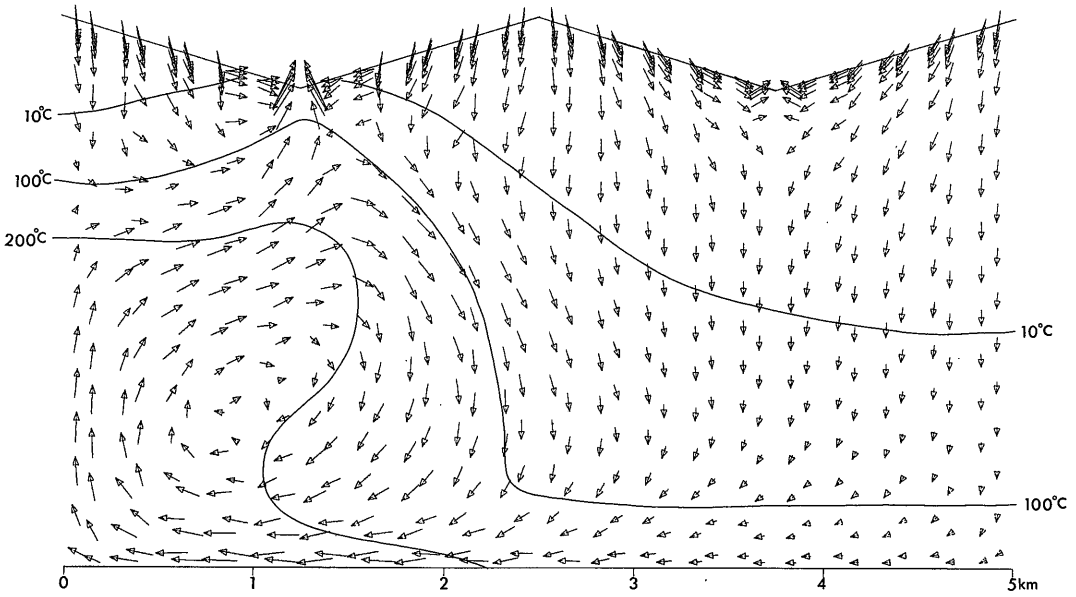

Fig. 7(1)

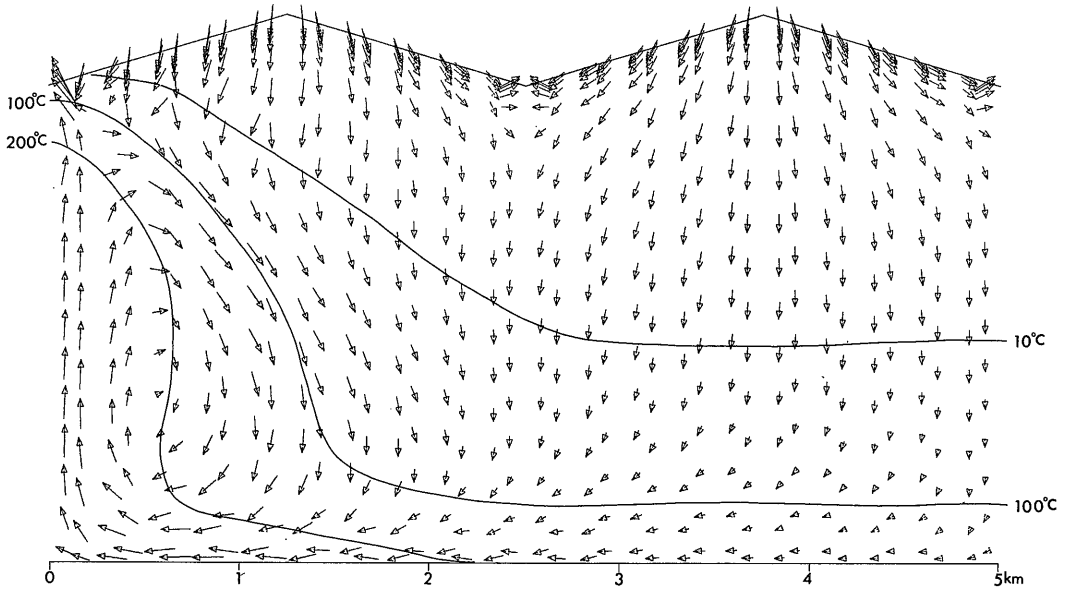

Fig. 7(2)

Fig. 7 Effects of mountain range with short wave length. (1) A mountain above heat source. (2) A valley above heat source.

column of buoyant flows. The cold down flow distinguishes itself by the straight line of no temperature gradient and the sharp temperature increase at the bottom as seen in the profiles 5 and 6. The profiles 3 and 4 are of the third type. The hot plume and the cold down flow are colliding at intermediate level forming steep temperature gradient. This means that it is not always necessary to assume an impermeable bed to interprete the third type of thermal logs.

Temperature reverse is caused by lateral flow. The Figure 5 (b) through (d) show the varied degree of effect of lateral flow. The influence of laterally spreading warm flow in upper strata and cooled return current at lower level are evident.

Figure 5 (e) shows the profiles near the side boundary on the right, where lateral flow is diminished. The vertical flows in this cases are gentle. So, the temperature gradient is moderate.

These temperature profiles have many features in common with field data from geothermal area. More extensive study of topographic effect on hydrothermal system will contribute to better interpretation of field data.

Some supplemental models are studied in the following discussion.

The model (5) of Figure 4 is modified to reduce the gradient of fluid potential which works on hydrothermal system. For this effect, a mountain with the same slope of gradient 18/100 is placed on the opposite side in Figure 6 (1), and water is introduced to the middle level of the mountain to form a lake in Figure 6 (2). The convection patterns have returned to the type of the basic state, and very similar to the models (3) and (4) in Figure 4. The strong out flow is observed at the valley or near the coast line. The isotherm of 100°C is pushed up toward these outlet.

The models in Figure 7 are another expression of topographic effect. The mountains are steep (gradient of 30/100) but have short wave length. They are shifted a half wave length each other for the model (1) and model (2). When there is a valley just above heat source, squeezing of reservoir occures in the model (2). So the hot zone becomes very slim even compared with the basic state of model (1) in Figure 4.

Conclusion

The topographic effect on hydrothermal system has been discussed. It acts both favorably and adversely for the formation of geothermal reservoir depending upon their geometry with respect to heat source. When a mountain of moderate slope is above the heat source, it works as a cap for hydrothermal system and helps to form a large geothermal reservoir with good amount of heat stored in it. But the convection system change suddenly to a dispersive type when the steepness of a mountain exceed a certain critical level. A valley above heat source expedite discharge of hot water. Shore line is another prefered place of discharge for thermal water.

Acknowledgement

Several helpful discussions with Dr. K. OGAWA and Mr. M. KAWAMURA are gratefully acknowledged. The author also would like to thank Dr. J. SUYAMA for his continuing encouragement.

References

DONALDSON, I. G. (1962) Temperature dradients in the upper layers of the earth's crust due to convective water flows. *J. geopys. Res.*, vol. 67, p. 3449–3459.

FAUST, C. R. and MERCER, J. W. (1979) Geothermal reservoir simulation 1, Mathematical models for liquid- and vaper-dominated hydrothermal systems. *Water Resour. Res.*, vol. 15, p. 23–30.

GUSTAFSSON, Y. (1966) The influence of topography on ground water formation, in ERIKSSON, E., GUSTAFSSON, Y. and NILSSON, K. ed.,

Ground water problems. Proceedings of the International Symposium held in Stockholm, Oct. 1966, p. 3–21, pergamon press, 1968.

HEALY, J. (1975) Geothermal fluids in zones of recent volcanism. in Proceedings Second United Nations Symposium on the Development and Use of Geothermal Resources, San Francisco, California, USA, 20–29 May, 1975, vol. 1, p. 415–422.

JSME (1968) *JSME Steam tables.* The Japan Society of Mechanical Engineers, Tokyo, 116p.

MERCER, J. W., PINDER, G. F. and DONALDSON, I. G. (1975) A Galerkin-finite element analysis of the hydrothermal system at Wairakei, New Zealand. *J. Geophys. Res.*, vol. 80, p 2608–2621.

ZINKIEWICZ, O. C. (1971) *The finite element method in engineering science* (translated to Japanese by M. KISHIKI *et al.*) Baifukan, Tokyo, 575p.

熱水系の数値モデル実験；地形の影響

花岡　尚之

要　旨

地熱探査には他の分野で発達した技術も含めて，多くの種類の調査が行われ，データが蓄積されている．これらのデータを総合し，一つの熱水系モデルにまとめる試みの一部として数値モデル実験を試みた．

浅い地温に地下水の流動が強い影響を及ぼしていることはよく知られている．HEALY (1975) は熱水系についても地下水の影響があることを模式的に示した．しかし，対流については考慮していない．

均質媒質内の熱水系に及ぼす地形の影響を調べるため，定常状態の熱エネルギー及び質量保存の微分方程式を有限要素法で解いた．ここで，地形は地下水面を表わすものとする．

熱源の上にある適当な高さの山は熱水系の蓋の役を果し，大きな熱を蓄える．しかし，山の高さがある臨界値を超えると，熱水の対流パターンは一変し，熱水系は発散的になる．

地形を考慮した数値モデルに見られる垂直温度分布は，中深度の温度の急上昇とか温度の逆転など，実測データに見られる特性を示している．これにより，温度検層データから熱水系の推定も可能となる．

（受付：1980年5月2日；受理：1980年5月12日）